euronoise

On the analysis of the time spreading of sound diffusers

Javier Redondo[a], Rubén Picó[b] and Mark Avis[c]

[a]IGIC - Universitat Politècnica de València, Cra. Nazaret-Oliva S/N, E-46730 Gandia, Spain
[b]EPSG - Univ. Politécnica de Valencia, c/ Nazaret-Oliva s/n, 46780 Grau de Gandia, Spain
[c]University of Salford, Acoustics Research Centre, Newton Building, M5 4WT Salford, UK
rpico@fis.upv.es

Since the invention of sound diffusers three decades ago a substantial effort has been made to predict the acoustic behaviour of these structures. BEM methods are well established for this purpose after a systematic comparison between simulations and experimental data. Volumetric methods such as Finite Element Methods (FEM) or the Finite Difference Time Domain method (FDTD) are not often used, due to their large computational cost. However, Near to Far Field Transformations (NFFT) can overcome that problem. Recently some of the authors have shown that the FDTD method is a useful technique to analyse the time domain signature of sound diffusers. In this paper a careful analysis of the performance of diffusers in the time domain ('time spreading') are reported, opening a new field of research.

1 Introduction

Sound scattering by a wall structure is an important factor affecting the sound quality of critical listening spaces. In recent years, significant efforts have been directed towards defining measurement techniques in order to characterize the performance of sound diffusers. In 1995 Mommertz and Vorländer [1, 5] presented a new technique for the characterization of sound diffusers, based on the incoherency of diffusely reflected sound. Two alternative methods were introduced; the free field method, illustrating the concept of using coherence to split the reflected sound into its specular and scattered components, and a reverberant method which exploits this principle more efficiently to get a random incidence coefficient. Both methods provide the '**scattering coefficient**'; that is, a measure of the proportion of sound energy not reflected in a specular manner. This coefficient is ideally suited for incorporating scattering into the current generation of geometric room acoustic models.

Both measurement techniques exploit certain time features of the scattered sound, and thus it is appropriate that a time domain technique should be used to simulate them. The Finite Difference Time Domain Method (FDTD) is increasingly popular in acoustics[3]. In this method, the equations are transformed to central-difference equations obtaining update formulations for the sound pressure and particle velocity. The main strength of FDTD relies on its being an extremely intuitive technique, so users can easily write and debug their own codes. The method can be easily implemented for room acoustics applications.

The object of this work is to produce a FDTD model for the direct prediction of the random-incidence scattering coefficient of sound diffusers, using a simulation of the measurements associated with the ISO standard. Results of simulations of the free field method will also be presented, to validate the numerical technique.

2 Numerical setup

2.1 FDTD scheme

The starting point of an acoustic FDTD model with no sound sources is given by the equations for conservation of momentum and continuity. In a homogeneous medium with no losses, these can be written as:

$$\frac{\partial p}{\partial t} + k\vec{\nabla}\cdot\vec{u} = 0 \qquad (1a)$$

$$\vec{\nabla}p + \rho_0 \frac{\partial \vec{u}}{\partial t} = 0 \qquad (1b)$$

where p is the pressure field, $\vec{u} = (u_x, u_y)$ is the vector particle velocity field, ρ_0 is the mass density of the medium and $k = \rho_0 c^2$ is the compressibility of the medium. The spatial and time derivatives of pressure and particle velocity can be approximated by central finite difference. For instance, the derivative of the sound pressure respect to x can be approximated as

$$\left.\frac{\partial p}{\partial x}\right|_{x=x_0} \approx \frac{p\left(x_0 + \frac{\Delta x}{2}\right) - p\left(x_0 - \frac{\Delta x}{2}\right)}{\Delta x} \qquad (2)$$

where Δx is the spatial interval between two closely-spaced points in the x direction. In two dimensions, three grids must be defined; one grid for pressure and two for the different particle velocity components. To minimize the significance of higher order terms in equation 3 below, those grids are 'staggered'. For instance, the mesh for the x component of the particle velocity is shifted a distance of $\Delta x/2$ with respect to the pressure mesh. The same applies for time meshing; the particle velocity meshes are shifted $\Delta t/2$ in time with respect to the pressure mesh. In doing so one can obtain a set of update equations to obtain the values of pressure and particle velocity after repetition for a given number of steps:

$$p_{i,j}^{n+½} = p_{i,j}^{n-½} - k\,\Delta t\left(\frac{ux_{i+½,j}^{n} - ux_{i-½,j}^{n}}{\Delta x} + \frac{uy_{i,j+½}^{n} - uy_{i,j-½}^{n}}{\Delta y}\right)$$

$$ux_{i+½,j}^{n+1} = ux_{i+½,j}^{n} - \frac{\Delta t}{\rho}\left(\frac{p_{i+1,j}^{n+½} - p_{i,j}^{n+½}}{\Delta x}\right) \qquad (3b)$$

$$uy_{i,j+½}^{n+1} = uy_{i,j+½}^{n} - \frac{\Delta t}{\rho}\left(\frac{p_{i,j+1}^{n+½} - p_{i,j}^{n+½}}{\Delta y}\right) \qquad (3c)$$

where the superscripts represent the time index, and the subscripts the spatial indices, namely:

$$p_{i,j}^{n+½} = p(i\,\Delta x, j\,\Delta y, (n+½)\,\Delta t) \qquad (4a)$$

$$ux_{i+½,j}^{n} = u_x((i+½)\,\Delta x, j\,\Delta y, n\,\Delta t) \qquad (4b)$$

$$uy^{n}_{i,j+½} = u_y(i\,\Delta x,(j+½)\,\Delta y,n\,\Delta t) \qquad (4c)$$

To ensure numerical convergence, the time step should be small enough to describe the wave propagation. The limit relationship between the spatial steps and the time step is given by the so-called Courant number, s, which in 2 dimensions can be defined as follows

$$s = c\Delta t\sqrt{\left(\frac{1}{\Delta x}\right)^2+\left(\frac{1}{\Delta y}\right)^2} \le 1 \qquad (5)$$

Another limitation of FDTD, common to other numerical techniques, results from the fact that the maximum element size used in discretization is determined by the frequency, with the sample criterion requiring four elements per wavelength. It has been shown in literature [33] that at least 10 elements per wavelength are required for adequate accuracy. Thus at high frequencies, a large numerical problem has to be solved. In this paper we will use a space step small enough to have accurate results up to 5kHz.

2.2 Free Field method

The numerical scheme is designed as described in the free field method proposed by Momertz and Vorländer in [1&2] to estimate the scattering coefficient (Figure 1). In the free field method a series of impulse responses are measured as the test sample is rotated. A linear average of all the time-domain impulse responses, one for each angle of incidence, is undertaken. The averaging process removes incoherent reflections, and leaves only the coherent (and thus specular) part.

In order to reproduce anechoic boundary conditions, a Perfectly Matched Layer (PML) [4] has been used at the boundaries to simulate free field conditions. The elements of the mesh have been chosen with an approximate size of 1 cm, and in order to operate with a Courant number as close to 1 as possible, the sampling frequency is in the region of 8.4 kHz. For frequencies above 8.4 kHz, numerical dispersion will be significant enough to mask the energy reflected from the domain boundary.

The excitation is introduced by a point source placed at the right hand side of the integration area. Sound propagates towards the diffuser, and is (potentially) scattered in all directions on reflection. As the original idea was to move the diffuser instead of rotating it, the specular reflection angle is not well-defined. Due to this we include 10 receiver locations placed in a line far from the test specimen. Time domain signals are recorded at those positions. Instead of using time windowing to separate incident and reflected sound, a reference calculation without test specimen is made; then the reflected sound is obtained by simply subtracting that reference condition from impulse responses measured with the test specimen in-place. This is equivalent, and much simpler, to using the Total Field to Scattering Field formulation [5].

Only 2D simulations are considered in this paper. This means that the exact procedure laid down in the ISO standard, in particular the rotation of the test specimen, can not be reproduced. Instead, in this paper the test specimen is translated from side to side.

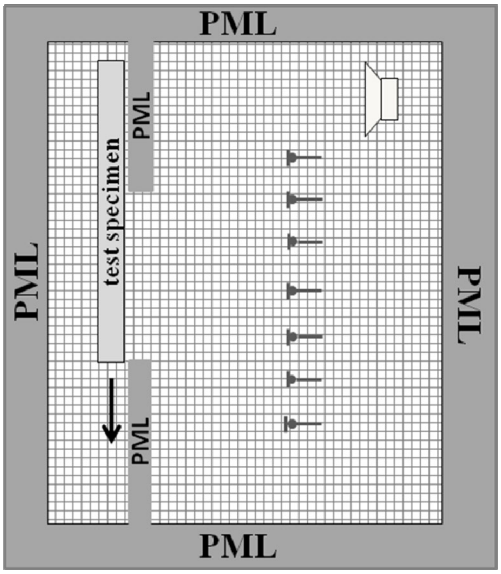

Fig.1 Numerical simulation of sound scattering following an adaptation of the Momertz and Vorländer free field method.

2.3 Reverberation chamber method

The basic idea of measuring scattering coefficients in a reverberation room is the same as described for the free field method. A circular test sample is introduced into a reverberant chamber, and impulse responses for different sample orientations are obtained. The initial parts of the reflections are highly correlated; these are the specular components of the reflection and remain unaltered as the sample is rotated. The latter parts of the impulse response, which are due to the scattering from the surface, depend strongly on the specific orientation.

Using synchronous averaging of these impulse responses, the diffuse reflected sound is cancelled out and a virtual impulse response containing only the specular energy is obtained. All the impulse responses used in this method are reverse-integrated to provide corresponding reverberation times, and a pseudo-absorption coefficient can be obtained in an analogous way to the Sabine method. Finally, a scattering coefficient is obtained from this pseudo-absorption coefficient and the more normal absorption coefficient.

The simulation scheme in for the simulations corresponding to the reverberant chamber method is represented in Figure 2. It is quite similar to the one of the free field method with the exception of the use of rigid terminations of the (reverberant) integration area.

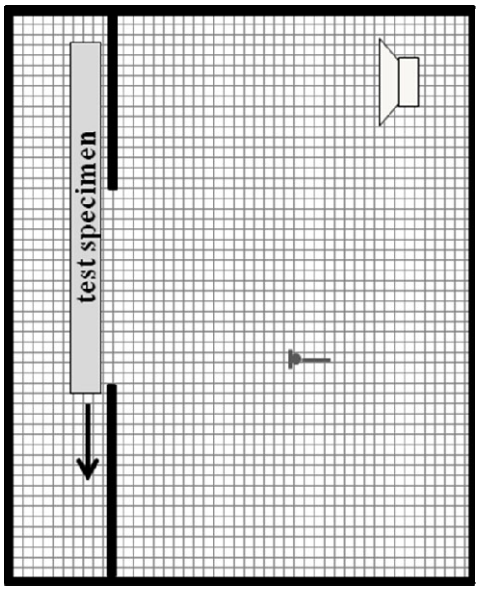

Fig.2 Numerical scheme simulation of sound diffusers following the ISO method in reverberant chamber.

effects.

3 Results

3.1 Free Field method

Figure 3 illustrates the band limited reflected pulses for one particular position of the sample and averaged for many sample positions. It can be observed that the initial parts of the reflections are highly correlated. These are the specular components of the reflection and remain unaltered as the sample is moved. In contrast, later parts are not in phase and depend on the particular position. By averaging the reflected pressure, the scattered component is removed and only the specular energy remains.

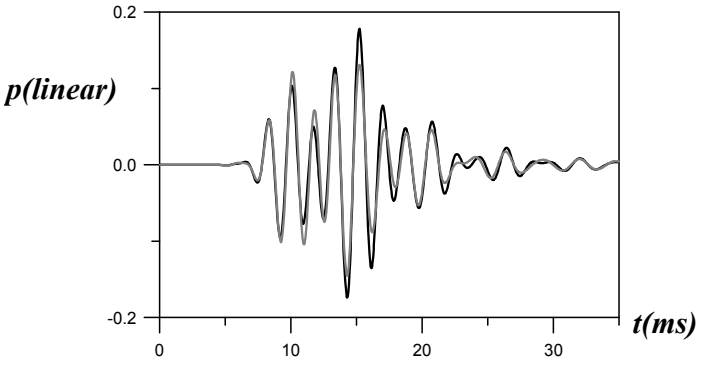

Fig.3 .- Band limited (1 octave centered at 500Hz) reflected pulses for one particular position of the sample (black line) and averaged for many sample positions (gray line). Set of triangles.

For validation purposes, the scattering coefficient is represented together with the correlation scattering coefficient [6]. The correlation coefficient has been obtained following the AES standard [7] to obtain the polar patterns of the reflected sound, and by using the equation:

$$\delta_c = 1 - \frac{\left|\sum_{i=1}^{n} p_1(\vartheta_i) p_2^*(\vartheta_i)\right|}{\sum_{i=1}^{n} |p_1(\vartheta_i)|^2 \cdot \sum_{i=1}^{n} |p_2(\vartheta_i)|^2} \quad (2)$$

where p_1 is the sound pressure reflected from the test specimen, p_2 is the sound pressure reflected from a flat panel, *denotes the complex conjugate, θ_i is the receiver angle of the i^{th} measurement position and *n* is the number of measurement positions.

The results are illustrated in Figure 4. Notice that the scattering coefficient for the diffuser does not drop back down to zero at low frequency but hovers around 0.2**.** This can be attributed to an effect of the proximity to the sample. In our reproduction of the Momertz and Vorländer method microphones are not in the far field for low frequencies.

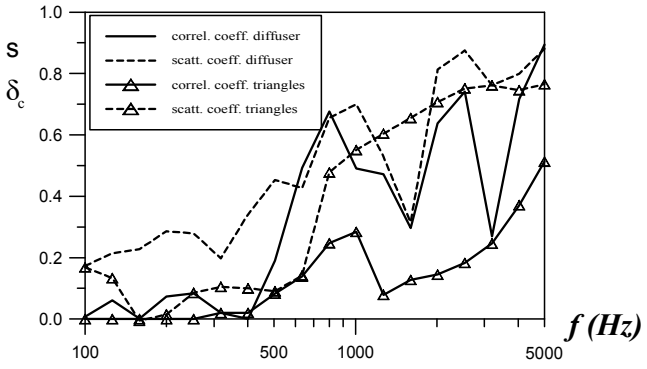

Fig.4 Normal incidence Scattering coefficient and correlation scattering coefficient of the tested surfaces vs frequency, evaluated with the Momertz and Vorländer free field method.

3.2 Reverberant chamber method

In figure 7 the impulse response of a single simulation is compared to the impulse response obtained after averaging several simulations with different positions of the test specimen. It can be observed that decay is slightly faster in the averaged case because of the removal of the diffusely reflected sound.

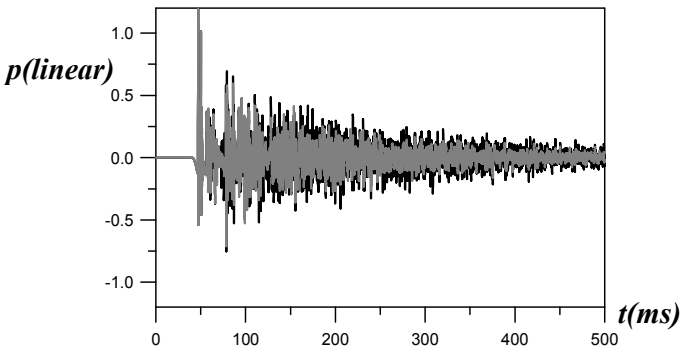

Fig.5 .- Impulse response of the room. Black line: one response. Gray line: Average of several impulses after translations of the test specimen

Figure 6 illustrates the results obtained following the above

method. It can be seen that the diffuser seems to be more efficient than the set of triangles. The fact that the scattering coefficient does not reach 1 at high frequencies, as generally observed in experimental data, can be attributed to two causes; on the one hand the numerical phase error is larger for high frequencies where the larger values of the scattering coefficient are expected. So the numerical noise can mask the decorrelation between signals. On the other hand, we have observed that for high frequencies the decays from the stationary state are no longer straight lines. Due to that the ranges used to estimate the reverberation time considered here has been different to the ones recommended in the ISO standard.

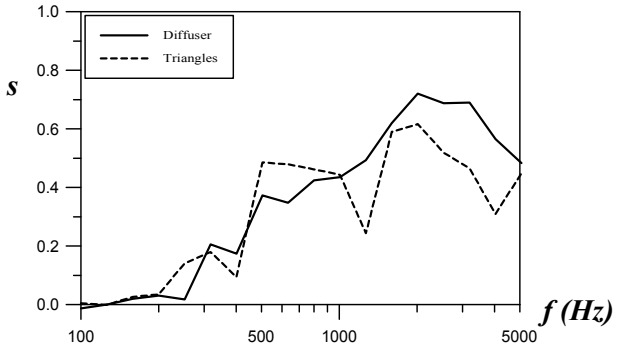

Fig. 6: Scattering coefficient of a diffuser, triangles and flat panel evaluated with the reverberant chamber method

4 Conclusion

A simple technique based on a FDTD scheme has been proposed to evaluate the random-incidence scattering coefficient of sound diffusers. Two methods have been tested the free field method and the reverberation chamber method. The normal incidence scattering coefficient and correlation scattering coefficient of different kind of diffusers like triangles or QRD have been analyzed.

References

[1] Mommertz E., Vorländer M., "Measurement of Scattering coefficient of surfaces in the reverberation chamber and in the free-field", Proceedings 15th ICA, Trondheim, 577-590 (1995)

[2] Vorländer M., Mommertz E., "Definition and Measurement of Random-incidence Scattering Coefficients", *Applied Acoustics* 60, 187-199 (2000).

[3] K. S. Yee, "Numerical solution of initial boundary value problems involving Maxwell's equations in isotropic media," IEEE *Transactions on Antennas Propag.*, 14, 302-7, (1966).

[4] X. Yuan, D. Borup, J. W. Wiskin, M,. Berggren, R. Eidens, S. Johnson, "Formulation and Validation of Berenger's PML Absorbing Boundary for the FDTD Simulation of Acoustic Scattering". *IEEE Transactions on Ultrasonics, Ferroelectrics, and Frequency control,* 44(4), 816-822, (1997)

[5] K. Umashankar and A. Taflove, ``A novel method to analyze electromagnetic scattering of complex objects," *IEEE Trans. Electromagnetic Compatibility*, 24, 397-405, (1982). [19] E. Mommertz, "Determination of scattering coefficients from reflection directivity of architectural surfaces," Applied Acoustics, 60(2), 201-204, (2000).

[6] E. Mommertz, "Determination of scattering coefficients from reflection directivity of architectural surfaces," Applied Acoustics, 60(2), 201-204, (2000).

[7] AES information document for room acoustics and sound reinforcement systems —Characterization and measurement of surface scattering uniformity. Audio Engineering Society. (2001)

[8] A. Farina. "Measurement of the surface scattering coefficient: comparison of the Mommertz/Vorländer approach with the new Wave Field Synthesis method". International Symposium on Surface Diffusion in Room Acoustics - Liverpool (GB) 16 April 2000